



Published in final edited form as:

Angiogenesis. 2011 September ; 14(3): 331–343. doi:10.1007/s10456-011-9217-1.

EAF2 loss enhances angiogenic effects of Von Hippel-Lindau heterozygosity on the murine liver and prostate

Laura E. Pascal,

Department of Urology, University of Pittsburgh School of Medicine, Suite G40, 5200 Centre Avenue, Pittsburgh, PA 15232, USA pascal@upmc.edu

Junkui Ai,

Department of Urology, University of Pittsburgh School of Medicine, Suite G40, 5200 Centre Avenue, Pittsburgh, PA 15232, USA aij@upmc.edu

Lora H. Rigatti,

Division of Laboratory Animal Resources, University of Pittsburgh Cancer Institute, University of Pittsburgh, Pittsburgh, PA 15261, USA rigattil@pitt.edu

Anne K. Lipton,

Department of Urology, University of Pittsburgh School of Medicine, Suite G40, 5200 Centre Avenue, Pittsburgh, PA 15232, USA liptonak@upmc.edu

Department of Pharmacology and Chemical Biology, University of Pittsburgh School of Medicine, Pittsburgh, PA, USA

Wuhan Xiao,

Department of Urology, University of Pittsburgh School of Medicine, Suite G40, 5200 Centre Avenue, Pittsburgh, PA 15232, USA w-xiao@ihb.ac.cn

Institute of Hydrobiology, Chinese Academy of Sciences, Wuhan 430072, People's Republic of China

James R. Gnarra, and

Department of Urology, University of Pittsburgh School of Medicine, Suite G40, 5200 Centre Avenue, Pittsburgh, PA 15232, USA gnarrarj@upmc.edu

Zhou Wang

Department of Urology, University of Pittsburgh School of Medicine, Suite G40, 5200 Centre Avenue, Pittsburgh, PA 15232, USA

Department of Pharmacology and Chemical Biology, University of Pittsburgh School of Medicine, Pittsburgh, PA, USA

Abstract

© The Author(s) 2011

Correspondence to: Zhou Wang.

wangz2@upmc.edu .

Electronic supplementary material The online version of this article (doi:10.1007/s10456-011-9217-1) contains supplementary material, which is available to authorized users.

Conflict of interest The authors indicate no potential conflicts of interest.

Open Access This article is distributed under the terms of the Creative Commons Attribution Noncommercial License which permits any noncommercial use, distribution, and reproduction in any medium, provided the original author(s) and source are credited.

Von Hippel-Lindau (VHL) disease results from the inactivation of the VHL gene and is characterized by highly vascular tumors. A consequence of VHL loss is the stabilization of hypoxia-inducible factor (HIF) alpha subunits and increased expression of HIF target genes, which include pro-angiogenic growth factors such as vascular endothelial growth factor (VEGF). In mice, homozygous deletion of VHL is embryonic lethal due to vascular abnormalities in the placenta; and, VHL^{+/-} mice develop proliferative vascular lesions in several major organs, most prominently the liver. Loss of ELL-associated factor (EAF2) in murine models has also been shown to induce increased vascular density in the liver as well as the prostate. Previously, EAF2 was determined to be a binding partner of VHL and loss of EAF2 induced a reduction in pVHL levels and an increase in hypoxia induced factor 1 α (HIF1 α) levels in vitro. Here we characterized the cooperative effects of VHL- and EAF2-deficiency on angiogenesis in the liver and prostate of male mice. VHL deficiency consistently increased the incidence of hepatic vascular lesions across three mouse strains. These vascular lesions were characterized by an increase in microvessel density, and staining intensity of VHL target proteins HIF1 α and VEGF. EAF2^{-/-}VHL^{+/-} mice had increased incidence of proliferative hepatic vascular lesions (4/4) compared to VHL^{+/-} (10/18) and EAF2^{-/-} (0/5) mice. Prostates of EAF2^{-/-}VHL^{+/-} mice also displayed an increase in microvessel density, as well as stromal inflammation and prostatic intraepithelial neoplasia. These results suggest that cooperation of VHL and EAF2 may be critical for angiogenic regulation of the liver and prostate, and concurrent loss of these two tumor suppressors may result in a pro-angiogenic phenotype.

Keywords

Von Hippel-Lindau (VHL); ELL-associated factor 2 (EAF2); Hepatic vascular lesion; Prostatic intraepithelial neoplasia (PIN)

Introduction

Von-Hippel-Lindau (VHL) gene inactivation results in a cancer syndrome characterized by tumors at various sites, including vascular tumors of the retinas and central nervous system, renal cancers, adrenal pheochromocytomas, and pancreatic tumors. The VHL protein (pVHL) is an E3 ubiquitin ligase that regulates hypoxia inducible factors alpha subunits (HIF1 α and HIF2 α) through targeted ubiquitination and proteasomal degradation under normoxic conditions [1–3]. Under hypoxic conditions pVHL levels are decreased [4] and HIF α subunits accumulate. The activated HIF transcriptional response results in expression of hundreds of genes whose products are involved in metabolism, cellular proliferation, and angiogenesis [5]. Although conventional deletion of VHL is embryonic lethal in the mouse due to placental vascular defects [6], conditional VHL deletions have been shown to induce hepatic vascular lesions [7–10], renal cysts [11] and pancreatic lesions [12].

Previously, we have shown that the androgen-responsive tumor suppressor ELL-associated factor 2 (EAF2) could block HIF-dependent angiogenesis by binding and stabilizing pVHL [13]. EAF2^{-/-} mice had reduced levels of pVHL in the testes; and mouse embryonic fibroblasts derived from EAF2^{-/-} mice had an increased activity and level of HIF1 α [13]. Furthermore, EAF2^{-/-} mice displayed an increase in blood vessel formation in the liver at 3 months of age [14]. These studies suggest that EAF2 may cooperate with VHL in the regulation of blood vessel formation and growth, and concurrent loss of function of VHL and EAF2 could contribute to a pro-angiogenic phenotype.

In order to further characterize the role of EAF2 and VHL in angiogenesis, we examined the effects of EAF2 loss and VHL heterozygosity in murine prostate and liver. Here we report that EAF2^{-/-}VHL^{+/-} mice had an increased incidence in hepatic vascular lesions as well as

increased liver and prostate vascularity compared to wild-type, EAF2^{-/-} and VHL^{+/-} mice. Increased vascularity in the liver was characterized by an increase in HIF1 α and VEGF immunoreactivity, particularly in hepatocytes near vascular lesions. In the prostates of EAF2^{-/-}VHL^{+/-} mice there was an increased incidence of PIN, stromal inflammation, fibrosis and smooth muscle proliferation compared to wild-type, EAF2^{-/-} and VHL^{+/-} mice.

Materials and methods

Generation of strain-specific VHL deletion mice

VHL^{+/-} mice [6] were generated by backcrossing to the BALB/c, FVB/N and C57BL/6 J strains (NCI Animal Production Facility, Frederick, MD, USA) for >12 generations to generate VHL^{+/-} mice with a pure background. Wild-type and VHL^{+/-} mice were maintained identically, under approval by the Institutional Animal Care and Use Committee of the Louisiana State University Health Sciences Center, New Orleans. Genotyping was determined by PCR analysis of mouse tail genomic DNA as described previously [6]. Mice were sacrificed at 12–15 mos of age.

Generation of EAF2 and VHL deletion mice on a C57Bl/6 background

Preparation of mice with specific deletion of EAF2 gene using HM1 embryonic stem cells has been described previously [14, 15]. EAF2^{+/-} mice were subsequently back-crossed to the C57BL/6 J strain (Jackson Laboratory, Bar Harbor, ME, USA) for >12 generations to generate EAF2^{-/-} mice with a pure C57BL/6 J background. EAF2^{-/-} VHL^{+/-} mice were generated from heterozygous intercrosses of EAF2^{+/-} and VHL^{+/-} mice (obtained from Dr. Laura Schmidt [8]) and subsequently from homozygous EAF2^{-/-}VHL^{+/-} intercrosses. Experimental cohorts were wild type, EAF2^{-/-}, VHL^{+/-}, and EAF2^{-/-}VHL^{+/-} male littermates. All mice were on a C57BL/6 background and were maintained identically, under approval by the Institutional Animal Care and Use Committee of the University of Pittsburgh. Genotyping was determined by PCR analysis of mouse tail genomic DNA as described previously [15]. Mice were sacrificed at 12–15 mos and 20–24 mos of age. Organs were cleaned of excess fat and membrane with phosphate-buffered saline and mass was determined by weighing after blotting with filtration paper to remove excess liquid. Prostate mass was determined as absolute mass as well as a ratio of organ to body mass to correct for body weight differences as described [16]. Samples were fixed in 10% formalin for at least 24 h, then embedded in paraffin, sectioned at 5 μ m, and stained with hematoxylin and eosin.

Immunohistochemistry

Immunohistochemical stains were performed on five-micron sections of paraffin blocks. Briefly, the sections of all groups were deparaffinized and rehydrated through a graded series of ethanol. Heat induced epitope retrieval was performed using 10 mmol/L of citrate buffer (pH 6), followed by rinsing in TBS buffer for 5 min. The primary antibodies (working dilution 1:400) were rat monoclonal anti-CD31 (MEC 13.3, 550274, BD Biosciences, San Jose, CA, USA), Ki-67 (TEC-3, M7249, Dako, Carpinteria, CA, USA), VHL (Ig32, 556347, BD Biosciences), HIF1 α (54, 610959, BD Biosciences), VEGF (P-20, sc-1836, Santa Cruz Biotechnology, Santa Cruz, CA, USA). Slides were then counterstained in hematoxylin and cover-slipped. Sections were imaged using a Zeiss Axioplan2 microscope and Axiovision Rel. 4.5 imaging software. Composite images were constructed with Photoshop CS (Adobe Systems, San Jose, CA). Extent of immunostaining was determined according to the presence or absence of specific staining when compared to positive and negative controls (Supplemental Figure 1). CD31-positive vessel density and Ki-67-positive cell density were determined by analysis of sections from at least 4 independent mice from each genotype. Assessment of microvessel density was determined based on CD31-positive blood vessel count as previously described [14]; proliferative index was determined based on cell count

as described [10]. Briefly, microvessel density was determined from at least 20 fields imaged at 10× magnification for prostate and 40× magnification for liver with no overlap and identified by evaluating histological sections, and CD31-positive vessels were counted to determine the average vessel numbers per field for each section. Proliferative index was determined from at least 20 fields imaged at 40× magnification with no overlap, Ki-67-positive cells were counted to determine the average number of proliferating cells for each section. All tissues were examined by an animal pathologist (L. Rigatti).

Cell culture and transfection

Primary mouse embryonic fibroblasts (MEF) were generated from embryonic day 12.5 (E12.5) to day 13.5 (E13.5) mixed C57BL/6 J/129 background embryos [13]. MEFs were maintained in DMEM with 10% fetal bovine serum (FBS), 0.1 mmol/L nonessential amino acids (Invitrogen), 100 μmol/L 2-mercaptoethanol (Sigma), and penicillin/streptomycin. MEFs were transfected using Lipofectamine 2000 (Invitrogen) in OPTI-MEM (Invitrogen). GFP-positive cells were sorted using flow cytometry. GFP-positive MEFs were then cultured in DMEM with 250 μM CoCl₂ to simulate hypoxia for 4 h, and cell lysates were collected for Western blot analysis. To control for variation, transfection experiments were repeated using several different clones.

Plasmids

The full length human EAF2 cDNA was subcloned into pEGFP-C1 vector (Clontech, Mountain View, CA, USA) to generate pEGFP-EAF2. In-frame cloning of the pEGFP-EAF2 fusion was verified by sequencing.

Western blot

Proteins were lysed in RIPA lysis buffer (50 mM Tris HCl pH7.4, 1% NP-40, 0.25% sodium-deoxycholate, 150 mM NaCl, 1 mM EDTA pH 8.0, 1 mM NaF) supplemented with 1 mM PMSF, 1 mM NaV₃O₄, and 1× protease inhibitor cocktail (P8340, Sigma–Aldrich, St Louis, MO, USA). Frozen livers were homogenized, and cells were placed on ice for 30 min and then centrifuged at 13,000g for 10 min at 4°C. Protein concentration was determined by BCA Protein Assay (Thermo Scientific, Rockford, IL, USA). Proteins (50 μg) from livers or whole cell MEF lysates were denatured and separated on a 10% SDS-polyacrylamide gel and transferred onto a nitrocellulose membrane. Blotted proteins were probed with antibodies as follows: mouse monoclonal anti-HIF1α antibody (1:2,000, 610958, BD Transduction Laboratories), rabbit polyclonal HIF1α (1:500, NB-100-449, Novus Biologicals, Littleton, CO, USA), rabbit polyclonal GFP (1:5,000, TP401, Torrey Pines Biolabs, Houston, TX, USA), rabbit polyclonal GAPDH (1:1,000, FL-335, sc-25778, Santa Cruz Biotechnology) and goat polyclonal β-actin (1:1,000, C-11, sc-1615, Santa Cruz Biotechnology), followed by horseradish peroxidase-conjugated secondary antibodies (Santa Cruz Biotechnology). Signals were visualized by enhanced chemiluminescence (ECL Western Blotting Detection Reagents, GE Healthcare) and were exposed to X-ray film (Fuji film, Valhalla, NY, USA). Membranes were stripped between antibody probes using a stripping solution (β-ME, 10% SDS, 0.375 M Tris pH 6.8).

Computational analysis of gene expression datasets from human prostate tissue specimens

Previously published datasets were queried for differential expression of CD31, EAF2 and VHL pathway genes VHL, HIF1A, HIF1AN (HIF1A inhibitor), VEGFA, VEGFB, and VEGFC in human prostate tissue specimens. Cell-type specific transcriptome profiles from normal prostate CD26⁺ luminal epithelial and CD49⁺ stromal cells [17] were compared to CD26⁺ cancer [18] and CD90⁺ cancer-associated fibroblasts [19]. The data were reported as

robust multi-array average (RMA) [20] normalized Affymetrix signal intensities implemented in an in-house analysis pipeline SBEAMS [21], or as a composite value: $X = \log_2(\text{Cancer normalized intensity; Normal normalized intensity})$.

Statistical analysis

Comparison between groups was calculated using the two-tailed Fisher's exact test method of summing small P values and the 1-way ANOVA and Bonferonni's Multiple Comparison Test as appropriate. The level of significance was set at $P = 0.05$. GraphPad Prism version 4 was used for graphics (GraphPad Software, San Diego, CA, USA). Values are expressed as means \pm SEM.

Results

VHL heterozygosity promotes the development of hepatic vascular lesions in a panel of murine strains

Mouse models from different genetic backgrounds often display variable phenotypes. We examined the incidence of vascular lesions in the liver induced by VHL heterozygosity in 3 inbred mouse strains: BALB/c, FVB/N and C57BL/6 at age 12–15 mos. Incidence of hepatic vascular lesions ranged from 33.3% in VHL^{+/-} FVB/N to 87.5% in VHL^{+/-} BALB/c mice (Fig. 1). Although there was variability in incidence across strains, no hepatic vascular lesions were detected in any of the wild-type mice examined, regardless of strain ($P < 0.05$). Therefore, in agreement with earlier studies [7–9], heterozygous pVHL inactivation is significantly associated with the development of hepatic vascular lesions.

EAF2 and VHL-deficiency cooperate to promote hepatic vascular lesions in C57BL/6 mice

To examine the potential cooperative effects of EAF2 and VHL in the development of hepatic vascular lesions, EAF2^{-/-}VHL^{+/-} mice on a C57BL/6 background were generated and compared to wild-type, EAF2^{-/-} and VHL^{+/-} mice. At ages 20–24 mos, all mice were sacrificed and organs were harvested, paraffin-embedded and sectioned for histological analysis. Histological analysis revealed several defects in the liver of VHL^{+/-} and EAF2^{-/-}VHL^{+/-} mice and prostates of EAF2^{-/-} and EAF2^{-/-}VHL^{+/-} mice (Table 1). The livers of wild-type and EAF2^{-/-} mice displayed no visible abnormalities at age 20–24 mos. However, 10 out of 18 (55.6%) VHL^{+/-} and 4 out of 4 (100%) EAF2^{-/-}VHL^{+/-} mice displayed large discrete lesions visible both on the surface of the liver and within the liver parenchyma (Fig. 2a). Histological analyses confirmed moderate to severe angiectasis in the VHL^{+/-} (10/18) and increased incidence of hepatic lesions in EAF2^{-/-}VHL^{+/-} (4/4, $P = 0.25$) mice (Fig. 2b). EAF2^{-/-}VHL^{+/-} mice also displayed increased focal thrombus formation, mild focal lymphocytic infiltration, hepatocyte loss, hepatic fibrosis and hepatocellular adenoma (Table 1).

Effects of EAF2 and VHL loss on prostate

Mice in all groups had similar body mass (Fig. 3a). Grossly, the prostates of all mice displayed no visible abnormalities at age 20–24 mos. Although not significant, there was an increase in prostate mass associated with EAF2-deficiency in line with previous reports (Fig. 3B, C) [15]. Histological analysis revealed several defects in the prostates of EAF2^{-/-} and EAF2^{-/-}VHL^{+/-} mice (Table 1, Fig. 3d, e). Compared to wild-type, EAF2^{-/-} mice displayed an increased incidence of prostatic intraepithelial neoplasia (PIN) (3/5), stromal fibrosis and fibroplasia and stromal edema. VHL^{+/-} mice displayed increased stromal inflammation, fibrosis and fibroplasia, but not PIN. One VHL^{+/-} mouse displayed lymphoma in the prostate. EAF2^{-/-}VHL^{+/-} mice displayed increased incidence of PIN (4/4), stromal inflammation (4/4), and stromal fibrosis and fibroplasia (4/4) (Fig. 3d, e). Mild multifocal

lymphocytic interstitial infiltrates were observed in all mice in all groups, possibly due to aging.

EAF2- and VHL-deficiency affects cellular proliferation in the murine prostate and liver

The proliferative marker Ki-67 was used to detect dividing cells in the prostate and liver of each genotype. In the prostate, the number of Ki-67-positive epithelial cells was significantly increased in EAF2^{-/-} and EAF2^{-/-}VHL^{+/-} mice as compared to wild-type or VHL^{+/-} mice (Fig. 4a, c). Since the number of Ki-67-positive cells was not significantly different between wild-type and VHL^{+/-} or between EAF2^{-/-} and EAF2^{-/-}VHL^{+/-} mice, this suggests that VHL loss does not affect epithelial cell proliferation in the prostate. In the liver, the number of Ki-67-positive cells was significantly increased in EAF2^{-/-}VHL^{+/-} mice compared to wild-type, EAF2^{-/-} and VHL^{+/-} mice (Fig. 4b, d). Loss of EAF2 or VHL alone did not significantly affect proliferation in the liver, suggesting that EAF2 and/or VHL may have tissue specific effects in regulation of cell proliferation in the prostate and the liver.

EAF2 and VHL gene deletion is associated with increased vascular density in the prostate and liver

To investigate the cooperative effects of EAF2 and VHL loss on microvessel density in the prostate and liver, we examined the number of CD31-positive blood vessels in both tissues by immunostaining (Fig. 5). We found that the number of CD31-positive vessels per field increased significantly in the prostates of EAF2^{-/-}, VHL^{+/-} and EAF2^{-/-}VHL^{+/-} mice as compared to wild-type control animals (Fig. 5c) and that CD31 staining increased in all lobes of the prostate (Fig. 5d). In the livers of these mice, the number of CD31-positive blood vessels increased significantly in EAF2^{-/-}VHL^{+/-} mice as compared to wild-type control animals. Although not statistically significant, the number of CD31-positive blood vessels was also increased in EAF2^{-/-} and VHL^{+/-} mice as compared to wild-type mice.

Effect of EAF2 and VHL deficiency on VHL pathway

Since HIF1 α is a target of VHL protein and VEGF is a HIF target, we evaluated the effects of EAF2 loss and VHL heterozygosity on expression of these products by immunostaining. In the prostate, blood vessels stained with HIF1 α in all groups (Fig. 6a). Increased nuclear immunoreactivity for HIF1 α has previously been reported in prostate intraepithelial neoplasia in human [22] and mouse tissue [23], however no epithelial HIF1 α expression was found in any groups in this study. A comparison of immunostaining intensity of HIF1 α -positive blood vessels showed an apparent additive increase in HIF1 α expression levels as well as the number of blood vessels in EAF2^{-/-}VHL^{+/-} prostates as compared to the prostates of wild-type, EAF2^{-/-} and VHL^{+/-} animals. In the livers of wild-type and EAF2^{-/-} animals, HIF1 α staining was confined to blood vessels and sinusoidal lining cells and hepatocytes displayed no immunoreactivity (Fig. 6b). Increased HIF1 α levels in the livers of EAF2^{-/-} animals at age 12 mos were shown by western blot analysis (Fig. 6c). In VHL^{+/-} animals, hepatocytes displayed positive cytoplasmic HIF1 α staining near portal areas. In EAF2^{-/-}VHL^{+/-} animals there was an apparent increase in cytoplasmic and rare nuclear HIF1 α staining of hepatocytes amid proliferating oval cells, particularly near vascular lesions. Increased nuclear and cytoplasmic expression of HIF1 α in hepatocytes has been associated with a response to hypoxic lesions in murine liver [24].

Previously we have shown that pVHL levels are reduced in EAF2^{-/-} mice, and endogenous HIF1 α protein levels are increased in immortalized EAF2^{-/-} MEFs under hypoxic conditions [13]. Here we show that transient transfection of GFP-EAF2 plasmids in EAF2^{-/-} MEF cells decreased HIF1 α protein levels, further substantiating a role for EAF2 in potentiating the degradation of HIF1 α under hypoxia (Fig. 6d).

HIF1 α is involved in the transcriptional regulation of pro-angiogenic stimulator VEGF [25], and increased expression of VEGF has been reported in prostate cancer and benign prostatic hyperplasia [26]. In the prostate, epithelial cells, stromal cells and blood vessels were positive for VEGF immunostaining, and no apparent changes were displayed among the groups (Fig. 7a). In the liver, hepatocytes and sinusoidal lining cells were positive for VEGF immunostaining. Increased VEGF expression in the extracellular space surrounding inflammatory cells and in hepatocytes has been reported in response to hypoxia [24]. EAF2^{-/-}VHL^{+/-} animals displayed areas of more intense VEGF immunostaining of hepatocytes, particularly near thrombus formations (Fig. 7b).

VHL expression has been reported in the basal epithelium of mice [27] and the basal and luminal epithelium of the human prostate [28]. In the prostates of wild-type and EAF2^{-/-} mice, VHL immunostaining was confined to the cytoplasm of epithelial cells, and there was no apparent difference in immunostaining pattern between these two groups (Fig. 8a). In VHL^{+/-} animals, there were random epithelial cells that were negative for VHL immunoreactivity; and in EAF2^{-/-}VHL^{+/-} prostates, some areas of PIN were negative for VHL immunoreactivity. In the liver, VHL immunostaining intensity in EAF2^{-/-} appeared to be decreased in comparison to wild-type animals, especially in areas of angiectasis (Fig. 8b). In the liver of VHL^{+/-} animals, areas near vascular lesions were characterized by VHL-negative proliferating oval cells and decreased VHL immunoreactivity in surrounding hepatocytes. In EAF2^{-/-}VHL^{+/-} animals, hepatic vascular lesions were surrounded by VHL-negative hepatocytes and proliferating oval cells whereas areas distal to the lesions were characterized by intense cytoplasmic VHL staining in multi-nucleated hepatocytes.

Differential expression of EAF2 and VHL pathway genes in human prostate cancer specimens

Previously published datasets from normal and cancer cells isolated from human prostate tissue specimens were queried for differential expression of CD31, EAF2 and VHL pathway genes VHL, HIF1A, HIF1AN, VEGFA, VEGFB, and VEGFC (Fig. 9). Cell-type specific comparison of cancer versus normal luminal epithelial cells and cancer-associated fibroblasts versus normal stromal cells showed that EAF2 was down-regulated in cancer. Additionally, CD31 and VHL pathway genes HIF1A, VEGFA and VEGFB were up-regulated in both cancer and cancer-associated fibroblasts, whereas VHL, HIF1AN and VEGFC were upregulated in cancer-associated fibroblasts but not cancer. These results from human tissue specimens correlate with the apparent increase found in the expression of HIF1 α and VEGF, and loss of VHL in EAF2^{-/-}VHL^{+/-} animals compared to wild-type. These data further suggest that EAF2 down-regulation may contribute to the development of an angiogenic phenotype in prostate disease.

Discussion

It has long been recognized that tumor angiogenesis is critical to tumor growth, survival and metastatic potential [29]. Microvessel density was been shown to be highly correlated with disease progression in both prostate [30] and hepatocellular carcinoma [31]. Loss of tumor suppressors VHL and EAF2 have individually been shown to induce pro-angiogenic phenotypes in murine models. VHL^{+/-} mice developed hepatic vascular lesions [7] and EAF2^{-/-} mice developed PIN lesions [15]. Furthermore, EAF2 has been shown to bind and stabilize pVHL, thereby inhibiting HIF-driven angiogenesis; and EAF2^{-/-} mice have reduced levels of pVHL in several major organs [13]. In the current study, combined deficiency of EAF2 and VHL led to a highly penetrant pro-angiogenic phenotype in the murine liver and prostate.

VHL deficiency consistently increased the incidence of hepatic vascular lesions across three mouse strains at ages >12 mos, and there seemed to be no significant discrepancies in the hepatic phenotype among different strains (Fig. 1). EAF2 deficiency increased the angiogenic effects of VHL heterozygosity in the murine liver. While not statistically significant ($P = 0.08$), EAF2^{-/-}VHL^{+/-} animals had a marked increase in the incidence of hepatic vascular lesions compared to VHL^{+/-} animals (100% vs. 55.6%) (Fig. 2). No lesions occurred in EAF2^{-/-} or wild-type mice. VHL or EAF2 deficiency alone had no effect on cellular proliferation in the liver (Fig. 4). Hepatic lesions in EAF2^{-/-}VHL^{+/-} mice displayed a statistically significant increase in proliferation compared to livers of EAF2^{-/-}, VHL^{+/-} and wild-type mice as measured by Ki-67 positive cells. The combined effects of EAF2 and VHL loss on proliferation were not seen in the prostate, however. Liver blood vessel formation determined by CD31 immunostaining was also significantly increased in EAF2^{-/-}VHL^{+/-} compared to the wild-type liver (Fig. 5). To a lesser degree, the livers of EAF2^{-/-} and VHL^{+/-} alone mice also displayed increased microvessel density which was consistent with previous reports [10, 14].

EAF2 deficiency has previously been shown to induce PIN in mice [15] and down-regulation of EAF2 expression has been reported in prostate cancer [15, 18]. VHL heterozygosity increased the incidence of PIN lesions in EAF2^{-/-} mice, from 60% in EAF2^{-/-} mice to 100% in EAF2^{-/-}VHL^{+/-} mice (Fig. 3). PIN lesions in EAF2^{-/-}VHL^{+/-} mice were accompanied by stromal inflammation, fibrosis and fibroplasia and smooth muscle proliferation and a statistically significant increase in microvessel density when compared to EAF2^{-/-}, VHL^{+/-} and wild-type mice.

Decreased pVHL expression has been reported in the affected tissues of VHL-deficient mice [8, 32, 33], due at least in part to the absence of one VHL allele. Rankin et al. [11] showed that renal tubule cysts, but not normal renal cortical cells exhibited biallelic VHL gene inactivation in VHL-conditionally deficient mice. We found lost or reduced pVHL expression in EAF2^{-/-}VHL^{+/-} in areas of PIN in the prostate and in angiectasis of the liver, suggesting that VHL inactivation was associated with the development of these lesions as well (Fig. 8). Loss or reduced pVHL expression could be the result of allelic loss. However, it could also occur through transcriptional or post-transcriptional mechanisms. It was not clear from our analyses whether pVHL loss was associated with a higher grade of PIN in EAF2^{-/-}VHL^{+/-} mice as compared to PIN seen in EAF2^{-/-} mice. Although VHL expression in the prostate epithelium has been reported previously [27, 28], the physiological role of the VHL gene in prostatic tissue remains to be elucidated.

Here we demonstrate that combined deficiency of VHL and EAF2 in mice increases angiogenesis in murine prostate and liver. Furthermore, this angiogenic phenotype was consistent with an increased incidence of pVHL-negative PIN and hepatic vascular lesions. The EAF2^{-/-}VHL^{+/-} mouse model demonstrates that these two tumor suppressors cooperate in the regulation of angiogenesis and that loss of these genes contributes to the development of neoplasia in the liver and prostate.

Supplementary Material

Refer to Web version on PubMed Central for supplementary material.

Acknowledgments

We are grateful to Ricardo Vencio and Julio Garcia for gene array data analyses and to Jianhua Xu, Aiyuan Zhang, Katie Leschak, Dawn Everard, Marie Acquafondata and Marianne Notaro for technical support. We also thank Dr. Laura Schmidt from NCI for providing VHL^{+/-} mice. This work was funded in part by grants T32 DK007774, R37 DK51193, R01CA120386, CA78335 and CA125930 (JG).

References

1. Maxwell PH, Wiesener MS, Chang GW, Clifford SC, Vaux EC, Cockman ME, Wykoff CC, Pugh CW, Maher ER, Ratcliffe PJ. The tumour suppressor protein VHL targets hypoxia-inducible factors for oxygen-dependent proteolysis. *Nature*. 1999; 399:271–275. [PubMed: 10353251]
2. Ohh M, Park CW, Ivan M, Hoffman MA, Kim TY, Huang LE, Pavletich N, Chau V, Kaelin WG. Ubiquitination of hypoxia-inducible factor requires direct binding to the beta-domain of the von Hippel-Lindau protein. *Nat Cell Biol*. 2000; 2:423–427. [PubMed: 10878807]
3. Rathmell WK, Simon MC. VHL: oxygen sensing and vasculogenesis. *J Thromb Haemost*. 2005; 3:2627–2632. [PubMed: 15975138]
4. Liu W, Xin H, Eckert DT, Brown JA, Gnarr JR. Hypoxia and cell cycle regulation of the von Hippel-Lindau tumor suppressor. *Oncogene*. 2010; 30:21–31. [PubMed: 20802534]
5. Hu CJ, Wang LY, Chodosh LA, Keith B, Simon MC. Differential roles of hypoxia-inducible factor 1alpha (HIF-1alpha) and HIF-2alpha in hypoxic gene regulation. *Mol Cell Biol*. 2003; 23:9361–9374. [PubMed: 14645546]
6. Gnarr JR, Ward JM, Porter FD, Wagner JR, Devor DE, Grinberg A, Emmert-Buck MR, Westphal H, Klausner RD, Linehan WM. Defective placental vasculogenesis causes embryonic lethality in VHL-deficient mice. *Proc Natl Acad Sci USA*. 1997; 94:9102–9107. [PubMed: 9256442]
7. Haase VH, Glickman JN, Socolovsky M, Jaenisch R. Vascular tumors in livers with targeted inactivation of the von Hippel-Lindau tumor suppressor. *Proc Natl Acad Sci USA*. 2001; 98:1583–1588. [PubMed: 11171994]
8. Ma W, Tessarollo L, Hong SB, Baba M, Southon E, Back TC, Spence S, Lobe CG, Sharma N, Maher GW, et al. Hepatic vascular tumors, angiectasis in multiple organs, and impaired spermatogenesis in mice with conditional inactivation of the VHL gene. *Cancer Res*. 2003; 63:5320–5328. [PubMed: 14500363]
9. Kleymenova E, Everitt JI, Pluta L, Portis M, Gnarr JR, Walker CL. Susceptibility to vascular neoplasms but no increased susceptibility to renal carcinogenesis in Vhl knockout mice. *Carcinogenesis*. 2004; 25:309–315. [PubMed: 14604887]
10. Chen S, Sanford CA, Sun J, Choi V, Van Dyke T, Samulski RJ, Rathmell WK. VHL and PTEN loss coordinate to promote mouse liver vascular lesions. *Angiogenesis*. 2010; 13:59–69. [PubMed: 20221685]
11. Rankin EB, Tomaszewski JE, Haase VH. Renal cyst development in mice with conditional inactivation of the von Hippel-Lindau tumor suppressor. *Cancer Res*. 2006; 66:2576–2583. [PubMed: 16510575]
12. Shen HC, Adem A, Ylaya K, Wilson A, He M, Lorang D, Hewitt SM, Pechhold K, Harlan DM, Lubensky IA, et al. Deciphering von Hippel-Lindau (VHL/Vhl)-associated pancreatic manifestations by inactivating Vhl in specific pancreatic cell populations. *PLoS One*. 2009; 4:e4897. [PubMed: 19340311]
13. Xiao W, Ai J, Habermacher G, Volpert O, Yang X, Zhang AY, Hahn J, Cai X, Wang Z. U19/Eaf2 binds to and stabilizes von hippel-lindau protein. *Cancer Res*. 2009; 69:2599–2606. [PubMed: 19258512]
14. Su F, Pascal LE, Xiao W, Wang Z. Tumor suppressor U19/EAF2 regulates thrombospondin-1 expression via p53. *Oncogene*. 2009; 29:421–431. [PubMed: 19826414]
15. Xiao W, Zhang Q, Habermacher G, Yang X, Zhang AY, Cai X, Hahn J, Liu J, Pins M, Doglio L, et al. U19/Eaf2 knockout causes lung adenocarcinoma, B-cell lymphoma, hepatocellular carcinoma and prostatic intraepithelial neoplasia. *Oncogene*. 2008; 27:1536–1544. [PubMed: 17873910]
16. Lindstedt L, Schaeffer PJ. Use of allometry in predicting anatomical and physiological parameters of mammals. *Lab Anim*. 2002; 36:1–19. [PubMed: 11833526]
17. Oudes AJ, Campbell DS, Sorensen CM, Walashek LS, True LD, Liu AY. Transcriptomes of human prostate cells. *BMC Genom*. 2006; 7:92.
18. Pascal LE, Vencio RZ, Page LS, Liebeskind ES, Shadle CP, Troisch P, Marzolf B, True LD, Hood LE, Liu AY. expression relationship between prostate cancer cells of Gleason 3, 4 and normal epithelial cells as revealed by cell type-specific transcriptomes. *Gene*. *BMC Cancer*. 2009; 9:452.

19. Pascal LE, Goo YA, Vencio RZ, Page LS, Chambers AA, Liebeskind ES, Takayama TK, True LD, Liu AY. Gene expression down-regulation in CD90 + prostate tumor-associated stromal cells involves potential organ-specific genes. *BMC Cancer*. 2009; 9:317. [PubMed: 19737398]
20. Irizarry RA, Hobbs B, Collin F, Beazer-Barclay YD, Antonellis KJ, Scherf U, Speed TP. Exploration, normalization, and summaries of high density oligonucleotide array probe level data. *Biostatistics*. 2003; 4:249–264. [PubMed: 12925520]
21. Marzolf B, Deutsch EW, Moss P, Campbell D, Johnson MH, Galitski T. SBEAMS-microarray: database software supporting genomic expression analyses for systems biology. *BMC Bioinform*. 2006; 7:286.
22. Zhong H, Semenza GL, Simons JW, De Marzo AM. Up-regulation of hypoxia-inducible factor 1alpha is an early event in prostate carcinogenesis. *Cancer Detect Prev*. 2004; 28:88–93. [PubMed: 15068831]
23. Huss WJ, Hanrahan CF, Barrios RJ, Simons JW, Greenberg NM. Angiogenesis and prostate cancer: identification of a molecular progression switch. *Cancer Res*. 2001; 61:2736–2743. [PubMed: 11289156]
24. Araujo AP, Frezza TF, Allegretti SM, Giorgio S. Hypoxia, hypoxia-inducible factor-1alpha and vascular endothelial growth factor in a murine model of *Schistosoma mansoni* infection. *Exp Mol Pathol*. 2010; 89:327–333. [PubMed: 20858486]
25. Carmeliet P, Dor Y, Herbert JM, Fukumura D, Brusselmans K, Dewerchin M, Neeman M, Bono F, Abramovitch R, Maxwell P, et al. Role of HIF-1alpha in hypoxia-mediated apoptosis, cell proliferation and tumour angiogenesis. *Nature*. 1998; 394:485–490. [PubMed: 9697772]
26. Lekas A, Lazaris AC, Deliveliotis C, Chrisofos M, Zoubouli C, Lapas D, Papatomas T, Fokitis I, Nakopoulou L. The expression of hypoxia-inducible factor-1alpha (HIF-1alpha) and angiogenesis markers in hyperplastic and malignant prostate tissue. *Anticancer Res*. 2006; 26:2989–2993. [PubMed: 16886625]
27. Nagashima Y, Miyagi Y, Udagawa K, Taki A, Misugi K, Sakai N, Kondo K, Kaneko S, Yao M, Shuin T. Von Hippel-Lindau tumour suppressor gene. Localization of expression by in situ hybridization. *J Pathol*. 1996; 180:271–274. [PubMed: 8958804]
28. Corless CL, Kibel AS, Iliopoulos O, Kaelin WG Jr. Immunostaining of the von Hippel-Lindau gene product in normal and neoplastic human tissues. *Hum Pathol*. 1997; 28:459–464. [PubMed: 9104946]
29. Folkman J. Tumor angiogenesis: therapeutic implications. *N Engl J Med*. 1971; 285:1182–1186. [PubMed: 4938153]
30. Weidner N, Carroll PR, Flax J, Blumenfeld W, Folkman J. Tumor angiogenesis correlates with metastasis in invasive prostate carcinoma. *Am J Pathol*. 1993; 143:401–409. [PubMed: 7688183]
31. Tanigawa N, Lu C, Mitsui T, Miura S. Quantitation of sinusoid-like vessels in hepatocellular carcinoma: its clinical and prognostic significance. *Hepatology*. 1997; 26:1216–1223. [PubMed: 9362365]
32. Iguchi M, Kakinuma Y, Kurabayashi A, Sato T, Shuin T, Hong SB, Schmidt LS, Furihata M. Acute inactivation of the VHL gene contributes to protective effects of ischemic preconditioning in the mouse kidney. *Nephron Exp Nephrol*. 2008; 110:e82–e90. [PubMed: 18957870]
33. Zanesi N, Mancini R, Seignani C, Vecchione A, Kaou M, Valtieri M, Calin GA, Pekarsky Y, Gnarr JR, Croce CM, et al. Lung cancer susceptibility in Fhit-deficient mice is increased by Vhl haploinsufficiency. *Cancer Res*. 2005; 65:6576–6582. [PubMed: 16061637]

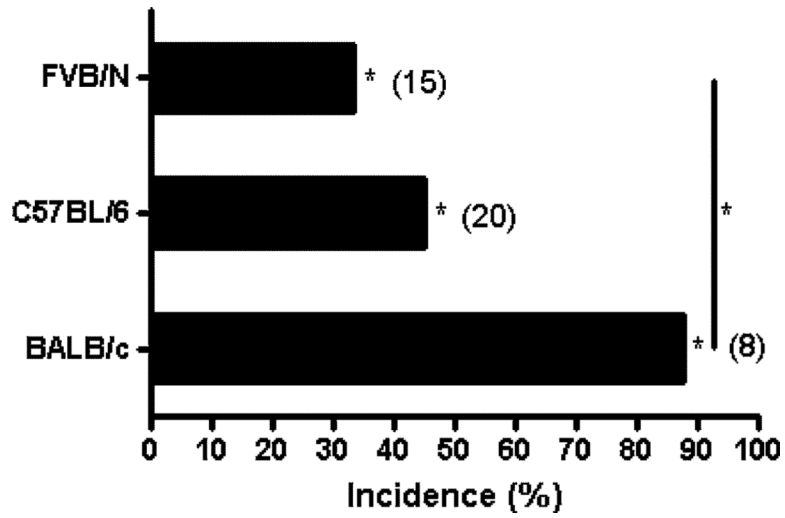


Fig. 1. Strain-specific incidence rate of hepatic vascular lesions in VHL^{+/-} mice at ages 12–15 mos. No hepatic vascular lesions were found in any wild-type control mice from each strain (**P* < 0.05)

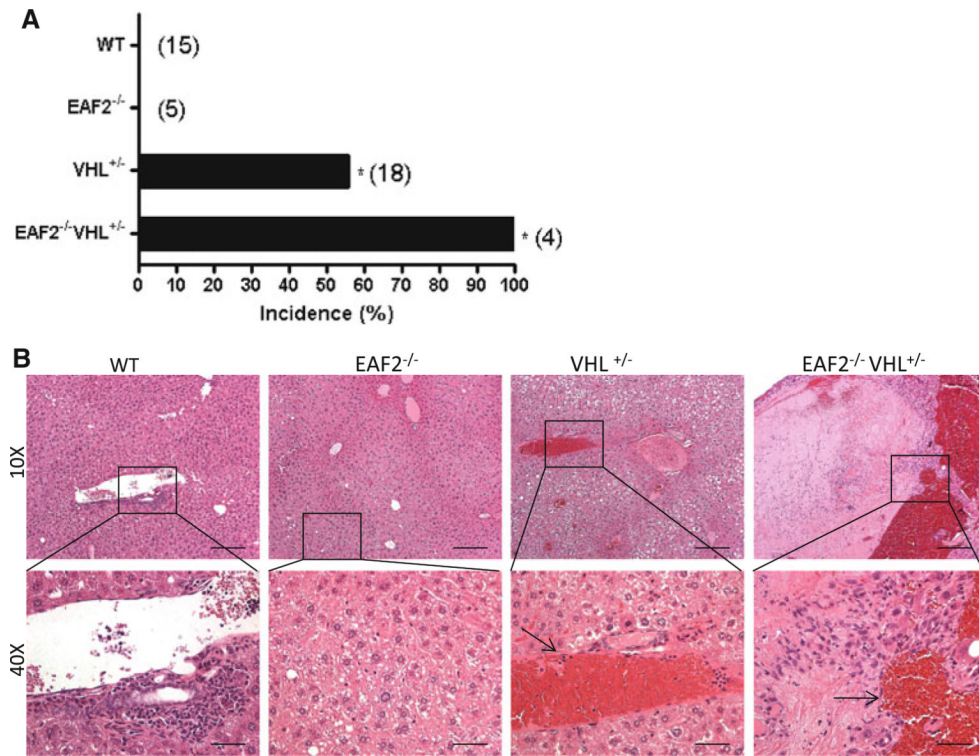


Fig. 2. Effect of combined EAF2- and VHL-deficiency on the incidence rate of hepatic vascular lesions at age 20–24 mos. (* $P < 0.05$). a Incidence rate of hepatic vascular lesions. b H&E stain of transverse sections of liver from wild-type control (WT), EAF2^{-/-}, VHL^{+/-} and EAF2^{-/-}VHL^{+/-} mice at age 20–24 mos. VHL^{+/-} and EAF2^{-/-}VHL^{+/-} livers displayed angiectasis (black arrows)

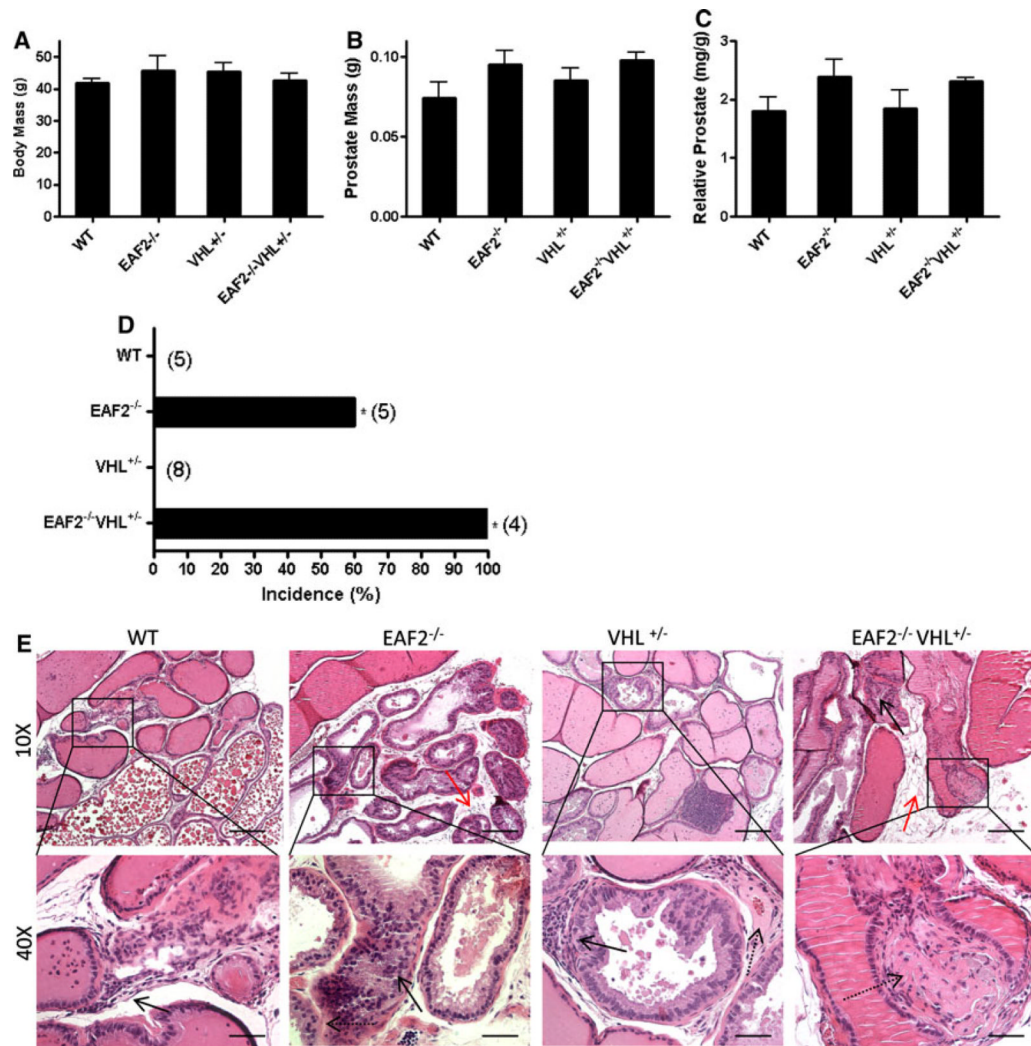


Fig. 3. Effect of combined EAF2- and VHL-deficiency on the prostate at age 20–24 mos. a Body mass. b Absolute prostate mass. c Relative prostate mass. Data represent average of 4–8 mice per group ($P > 0.05$). d Incidence rate of prostatic intraepithelial neoplasia ($*P < 0.05$). e H&E stain of transverse sections of prostate ventral lobes from wild-type control (WT), EAF2^{-/-}, VHL^{+/-} and EAF2^{-/-}VHL^{+/-} mice at age 20–24 mos. All groups displayed increased lymphocytic infiltration (*black arrow*, WT inset). EAF2^{-/-} mice displayed prostatic intraepithelial neoplasia (*black arrow*), stromal fibrosis and fibroplasia (*dashed arrow*) and stromal edema (*red arrow*). VHL^{+/-} mice displayed lymphocytic infiltration (*black arrow*), stromal fibrosis and fibroplasia (*dashed arrow*), but not prostatic intraepithelial neoplasia. EAF2^{-/-}VHL^{+/-} mice displayed prostatic intraepithelial neoplasia (*black arrow*), stromal fibrosis and fibroplasia (*dashed arrow*) and stromal edema (*red arrow*)

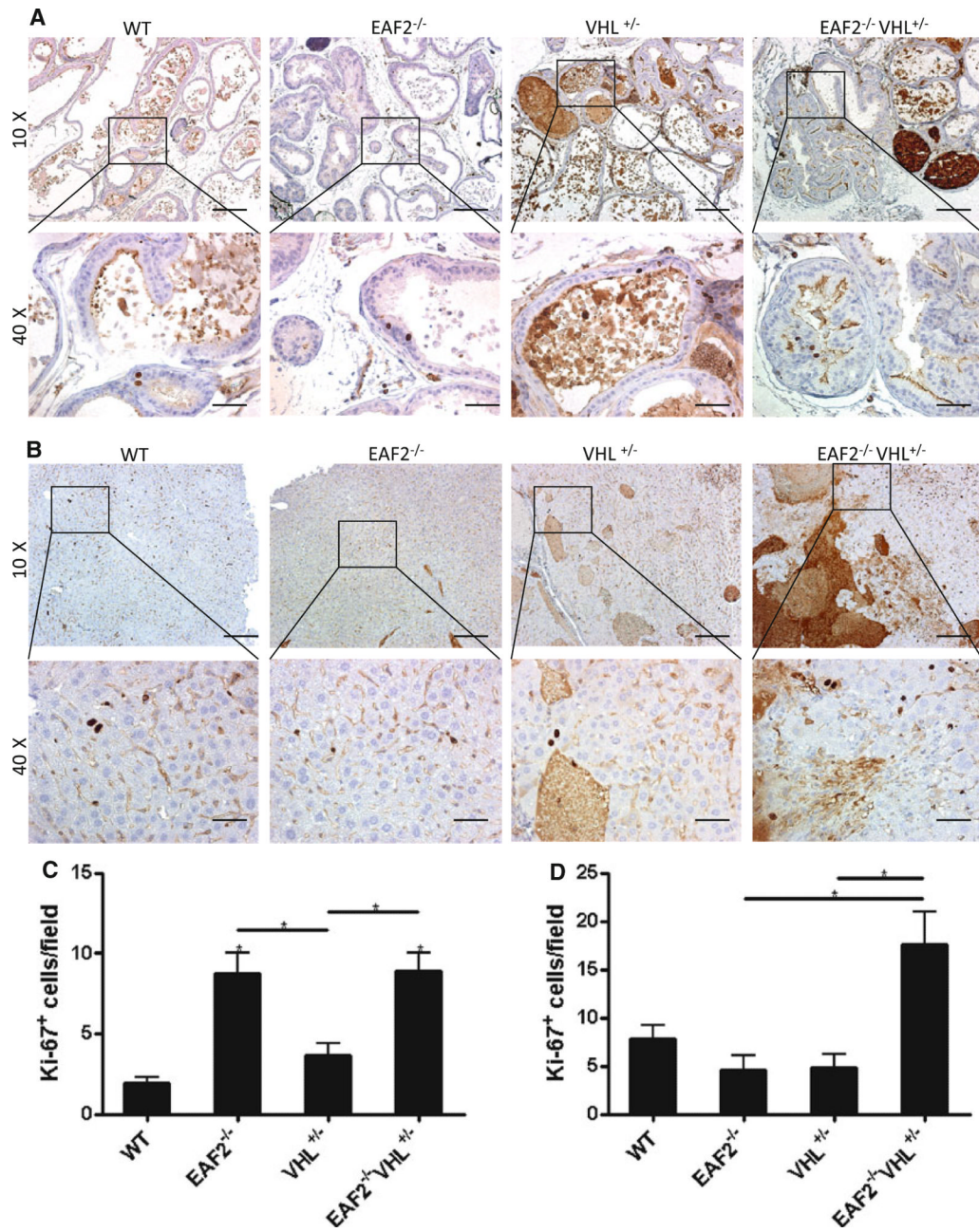
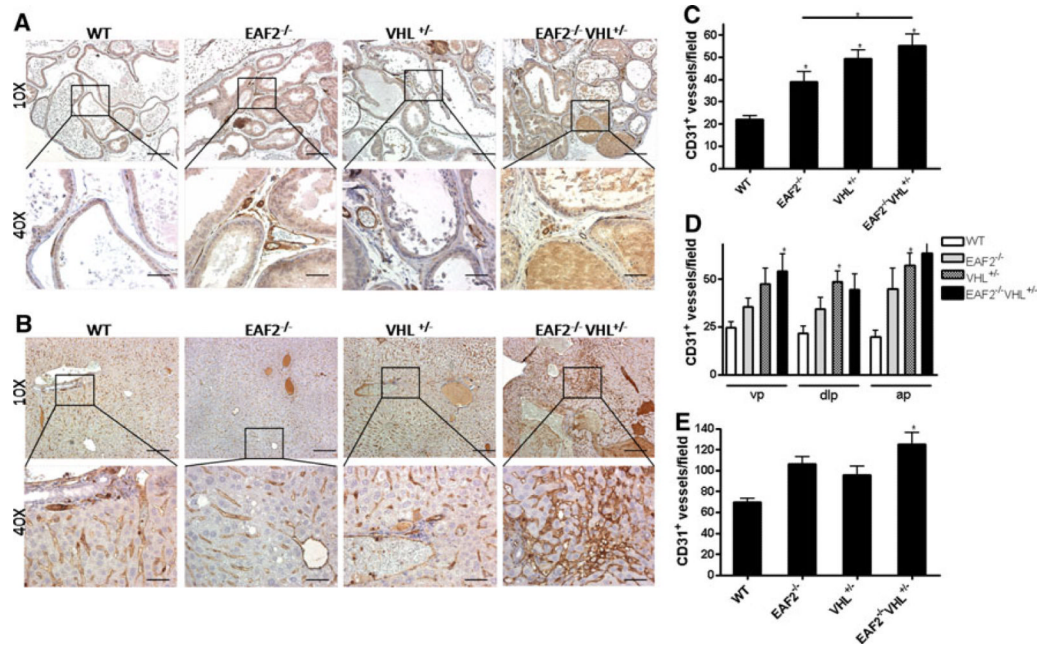


Fig. 4. Effects of EAF2- and VHL-deficiency on cellular proliferation in the prostate and liver. a Ki-67 immunostaining in transverse sections of prostate ventral lobes from wild-type control (WT), EAF2^{-/-}, VHL^{+/-} and EAF2^{-/-}VHL^{+/-} mice at age 20–24 mos. b Ki-67 immunostaining in transverse sections of liver from WT, EAF2^{-/-}, VHL^{+/-} and EAF2^{-/-}VHL^{+/-} mice at age 20–24 mos. Original magnification $\times 10$, inset $\times 40$. Scale bars indicate 200 μ m in $\times 10$, 50 μ m in $\times 40$. c Quantification of Ki-67⁺ epithelial cells in ventral prostate. d Quantification of Ki-67⁺ cells in liver. Data represent average of 4–8 mice per group (* $P < 0.05$)

**Fig. 5.**

Cooperative effects of EAF2- and VHL-deficiency on CD31⁺ blood vessel formation in the prostate and liver. a CD31 immunostaining of vessels in transverse sections of prostate ventral lobes from wild-type control (WT), EAF2^{-/-}, VHL^{+/-} and EAF2^{-/-}VHL^{+/-} mice at age 20–24 mos. b CD31 immunostaining in transverse sections of liver from WT, EAF2^{-/-}, VHL^{+/-} and EAF2^{-/-}VHL^{+/-} mice at age 20–24 mos. Original magnification $\times 10$, *inset* $\times 40$. *Scale bars* indicate 200 μ m in $\times 10$, 50 μ m in $\times 40$. c Quantification of CD31⁺ vessels in prostate. d Quantification of CD31⁺ vessels in the ventral (vp), dorsal-lateral (dlp) and anterior (ap) prostate. e Quantification of CD31⁺ vessels in the liver. Data represent average of 5–8 mice per group (* $P < 0.05$)

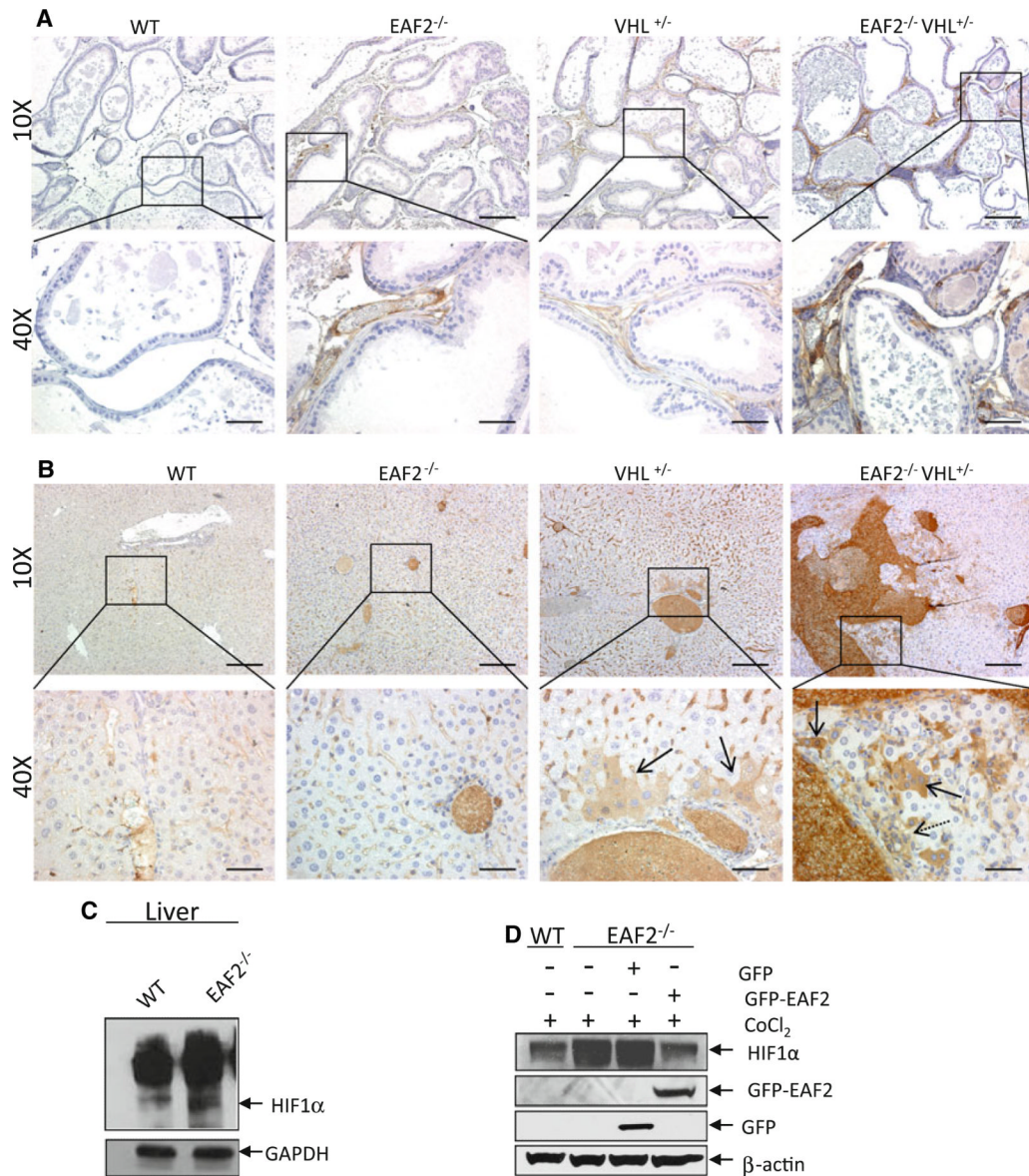


Fig. 6. Expression of HIF1 α in prostate and liver. a HIF1 α immunostaining of vessels in transverse sections of prostate ventral lobes from wild-type control (WT), EAF2^{-/-}, VHL^{+/-} and EAF2^{-/-}VHL^{+/-} mice at age 20–24 mos. b HIF1 α immunostaining of vessels in transverse sections of liver from wild-type control (WT), EAF2^{-/-}, VHL^{+/-} and EAF2^{-/-}VHL^{+/-} mice at age 20–24 mos. VHL^{+/-} mice displayed cytoplasmic staining of hepatocytes and sinusoidal lining cells proximal to portal areas (*black arrow*). EAF2^{-/-}VHL^{+/-} mice displayed cytoplasmic staining of hepatocytes and sinusoidal lining cells (*black arrows*) in areas of increased oval cell proliferation (*dashed arrow*). c Western blot analysis of HIF1 α expression in liver extracts of wild-type or EAF2^{-/-} mice at age 12 mos. Blots were reprobbed with GAPDH antibody to confirm equal protein loading. d Modulation of HIF1 α expression by EAF2 in MEF cells. EAF2^{-/-} MEF cells transfected with GFP-EAF2 had reduced HIF1 α expression. Blots were reprobbed with β -actin antibody to confirm equal protein loading. Western blot images are representative of at least 3 experiments

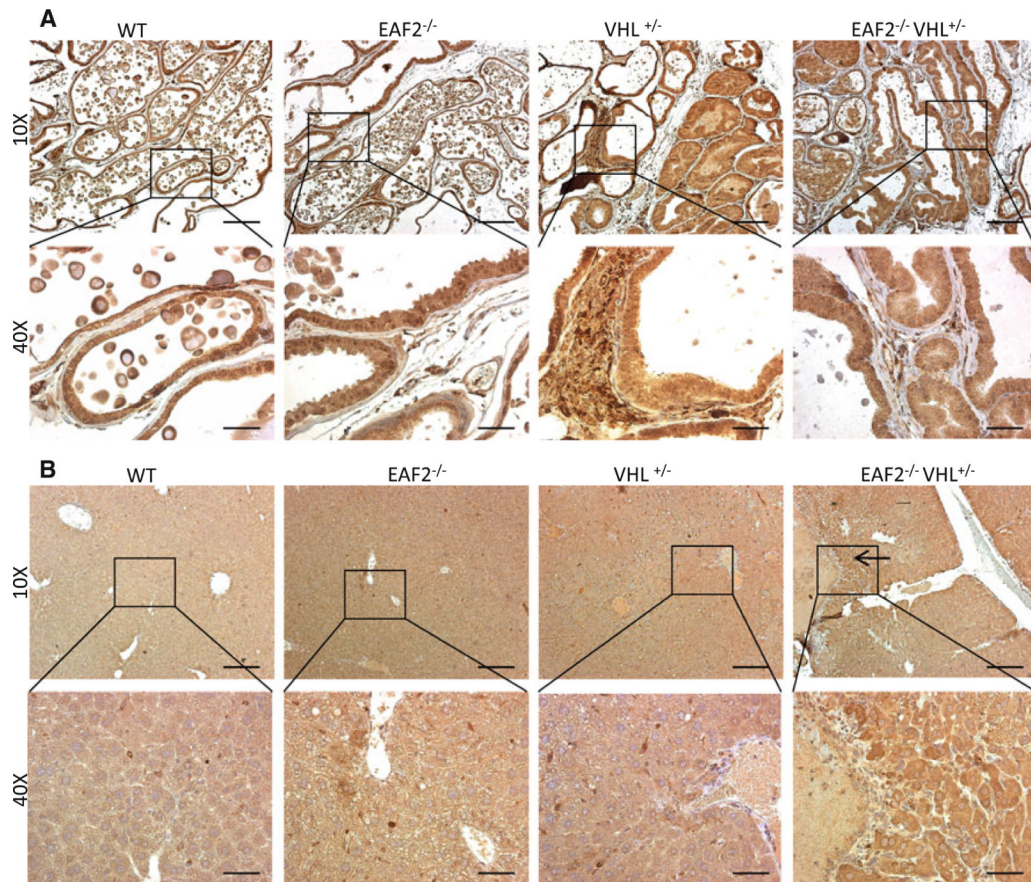


Fig. 7. Expression of VEGF in prostate and liver. a VEGF immunostaining in transverse sections of prostate ventral lobes from wild-type control (WT), EAF2^{-/-}, VHL^{+/-} and EAF2^{-/-}VHL^{+/-} mice at age 20–24 mos. b VEGF immunostaining of in transverse sections of liver from wild-type control (WT), EAF2^{-/-}, VHL^{+/-} and EAF2^{-/-}VHL^{+/-} mice at age 20–24 mos. EAF2^{-/-}VHL^{+/-} mice displayed areas of intense cytoplasmic staining of hepatocytes (*black arrow*)

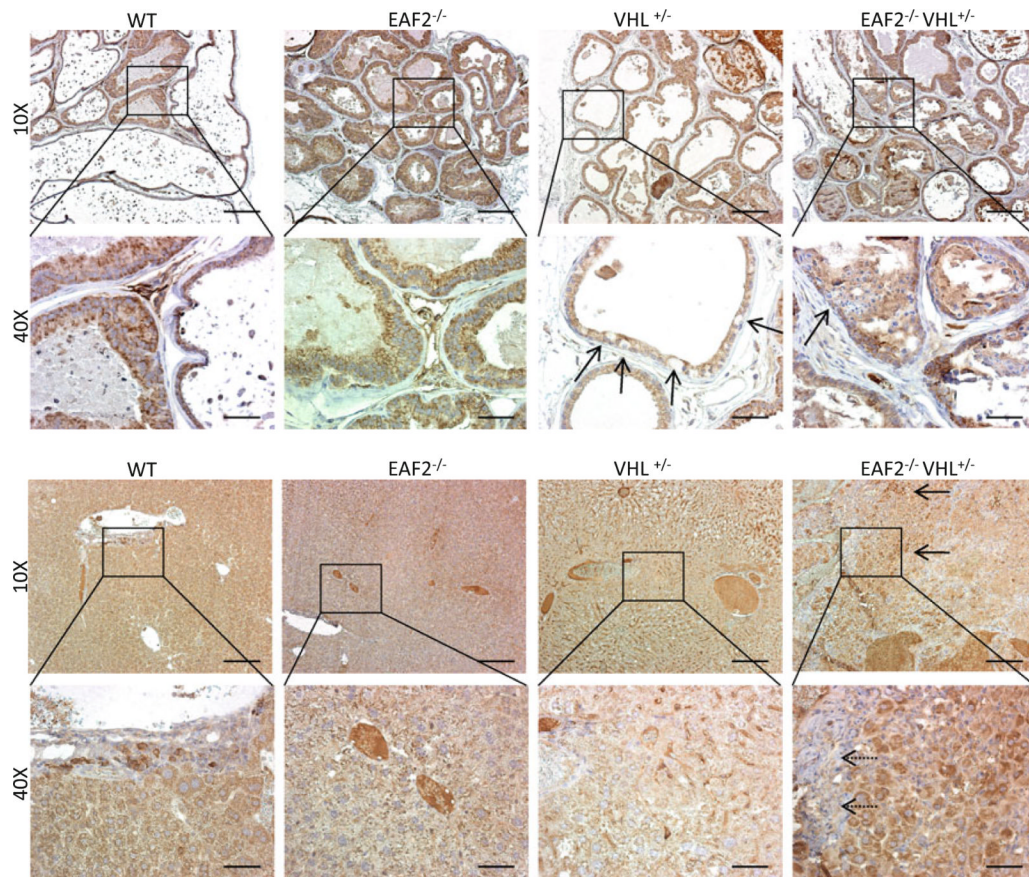


Fig. 8.

Expression of VHL in prostate and liver. a VHL immuno-staining in transverse sections of prostate ventral lobes from wild-type control (WT), EAF2^{-/-}, VHL^{+/-} and EAF2^{-/-}VHL^{+/-} mice at age 20–24 mos. VHL^{+/-} mice displayed sporadic negative VHL immunoreactivity (*black arrows*), and EAF2^{-/-}VHL^{+/-} mice displayed negative VHL immunoreactivity in PIN lesions (*black arrow*). b VHL immunostaining of in transverse sections of liver from wild-type control (WT), EAF2^{-/-}, VHL^{+/-} and EAF2^{-/-}VHL^{+/-} mice at age 20–24 mos.

Proliferating oval cells near areas of angiectasis in VHL^{+/-} animals were negative (*black arrow*) and surrounding hepatocytes had reduced VHL immunoreactivity. EAF2^{-/-}VHL^{+/-} mice displayed areas of intense cytoplasmic staining of hepatocytes (*black arrows*) and negative VHL immunoreactivity in proliferating oval cells and hepatocytes (*inset, dashed arrow*) near areas of angiectasis

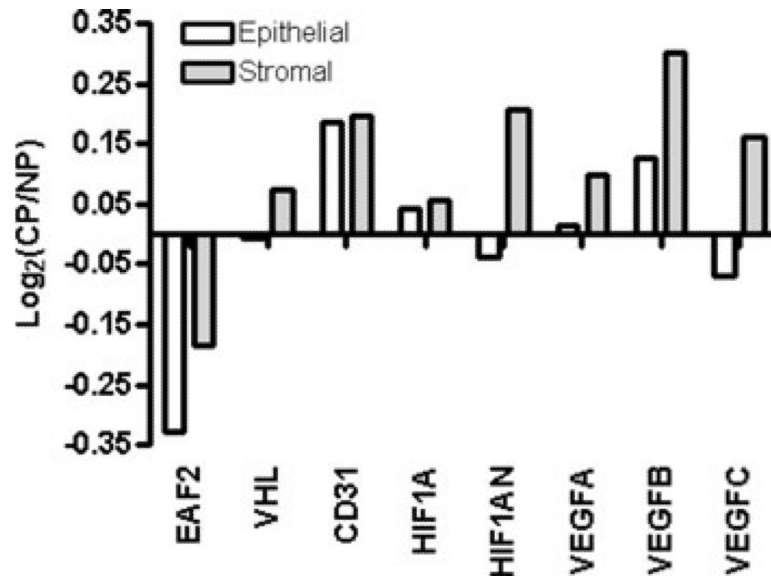


Fig. 9. Expression profile of EAF2 and VHL pathway genes in prostate cancer and cancer-associated fibroblasts compared to normal prostate epithelial and stromal cells as determined by analysis of sorted CD26⁺ (cancer and normal epithelial) cells, CD90⁺ (cancer-associated fibroblast) cells and CD49a⁺ (normal stromal) from human tissue specimens. Positive log₂ (Cancer/Normal) on the y-axis indicates increased cancer expression while negative log₂ indicates decreased cancer expression

Table 1Effects of VHL-deficiency on EAF2^{+/+} and EAF2^{-/-} mice at 20–24 mos

Phenotype	VHL ^{+/+}		VHL ^{+/-}	
	EAF2 ^{+/+}	EAF2 ^{-/-}	EAF2 ^{+/+}	EAF2 ^{-/-}
<i>Liver</i>				
Vascular lesions and mild-severe angiectasis			10	4
Focal thrombus formation				2
Fatty change—moderate		1	1	1
Hepatocellular adenoma				1
Focal lymphocytic infiltrate				1
Hepatocyte loss				1
Hepatic fibrosis				1
Extramedullary hematopoiesis			1	
Chronic portal infiltrates	1		1	
Number of mice examined	15	5	18	4
<i>Prostate</i>				
Prostatic intraepithelial neoplasia	0	3	0	4
Lymphocytic interstitial infiltrates	5	5	8	4
Ductal mucus plug				1
Lymphoma			1	
Stromal inflammation	2	2	4	4
Stromal edema				
Stromal fibrosis and fibroplasia, and smooth muscle proliferation	1	3	3	4
Number of mice examined	5	5	8	4